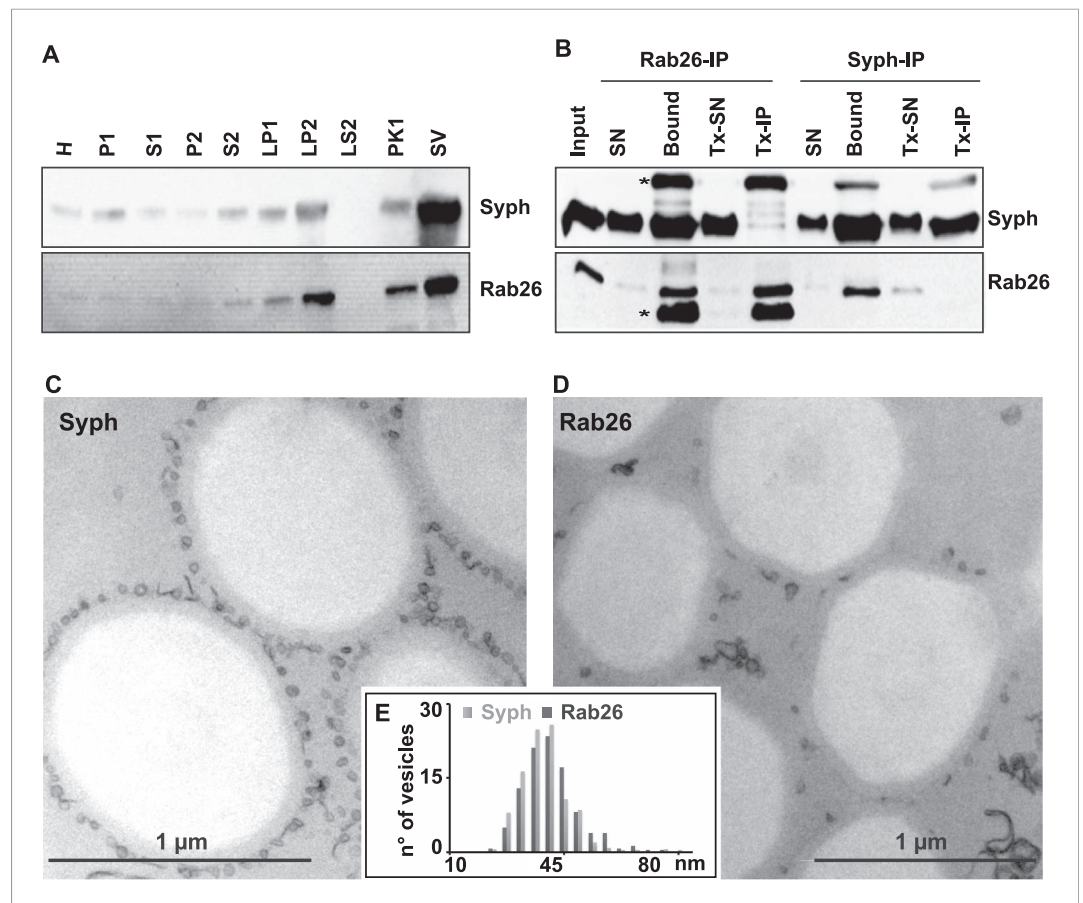


---

## Figures and figure supplements

The GTPase Rab26 links synaptic vesicles to the autophagy pathway

**Beyenech Binotti, et al.**



**Figure 1.** The small GTPase Rab26 co-purifies with synaptic vesicles. **(A)** Rab26 co-purifies with synaptic vesicles using conventional fractionation. Synaptic vesicles were purified from rat brain homogenate (H) by two consecutive differential centrifugation steps, yielding a low-speed pellet (P1) and a supernatant (S1), followed by a second centrifugation yielding a pellet P2 (containing synaptosomes and mitochondria) and a supernatant (S2). P2 was then lysed by osmotic shock, followed by centrifugation to separate large particles including synaptic junctional complexes (LP1) and a supernatant from which small membranes enriched in synaptic vesicles are collected by high-speed centrifugation (LP2, supernatant LS2 only contains soluble proteins). LP2 was further fractionated by sucrose density gradient centrifugation followed by chromatography on controlled pore glass beads where larger membrane fragments (PK1) were separated from synaptic vesicles (SV) (Huttner et al., 1983). 12  $\mu$ g of proteins of each fraction was analyzed by SDS-PAGE and immunoblotting for Rab26 and the synaptic vesicle marker synaptophysin. Note that Rab26 copurifies with synaptophysin, displaying a pattern typical of synaptic vesicle proteins. **(B)** Synaptic vesicles were immunoprecipitated using Eupergit C1Z/methacrylate beads to which monoclonal antibodies specific for Rab26 or synaptophysin (Syph) respectively, were covalently coupled. The beads were incubated with a resuspended LP2 fraction and collected (see [Burger et al., 1989; Takamori et al., 2000] for details). SN, supernatant obtained after bead incubation; Bound, immunisolates; Tx-SN and Tx-IP, same as before but the Input sample was solubilized with Triton X-100 to a final concentration of 1% before immunoprecipitation. For immunoblotting, 4% of the input or supernatant samples and 33% of bound samples were loaded for analyses. Note that Rab26 and synaptophysin cofractionate with the immunobeads irrespective of the antibody employed. Incubation with synaptophysin beads quantitatively depleted Rab26 from the supernatant whereas depletion of synaptophysin by Rab26-beads was less complete. In contrast, only the respective antigen was recovered from the detergent-solubilized samples. Asterisks denote IgG heavy and the light chains of the antibodies used for isolation, respectively. **(C and D)** Electron microscopy showing ultrathin sections of methacrylate beads containing bound organelles that were captured with synaptophysin- **(C)** or Rab26-specific **(D)** antibodies, respectively. **(E)** Size distribution (diameter) of bead-associated vesicles. Note that both populations exhibit a very similar and homogeneous size distribution, with a peak between 40–45 nm as is characteristic for synaptic vesicles (Takamori et al., 2006).

DOI: 10.7554/eLife.05597.003

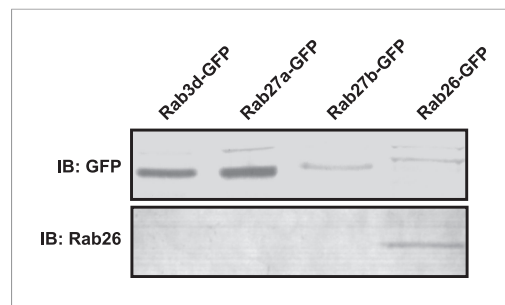


**Figure 1—figure supplement 1.** Monoclonal Rab26 antibody generated in this study specifically recognizes Rab26. 10 mg of lysates from NIH 3T3 cells transiently transfected with GFP-tagged versions of Rab3d, Rab27a, Rab27b or Rab26 were immunoblotted and probed with anti-GFP (upper panel) or the monoclonal anti-Rab26 (lower panel) antibodies. The newly generated monoclonal antibody recognizes only Rab26 but does not react with the other closely related Rab proteins.

DOI: [10.7554/eLife.05597.004](https://doi.org/10.7554/eLife.05597.004)

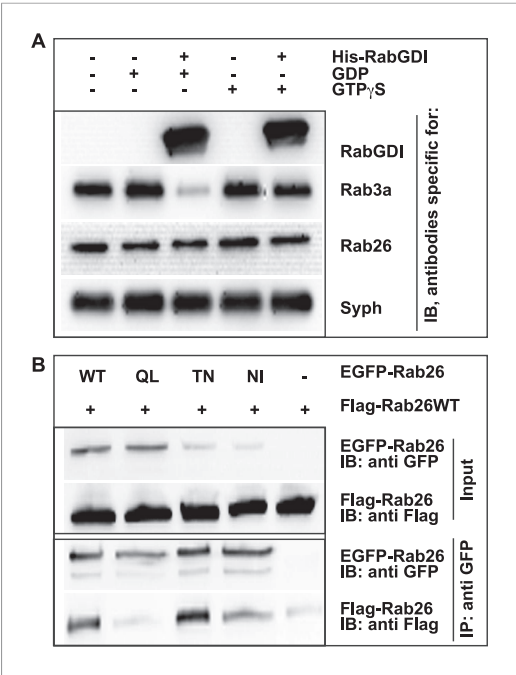


**Figure 2.** GDP-Rab26 cannot be extracted by GDI from membranes and forms oligomers. **(A)** Rab26 is resistant to extraction by GDI from synaptic vesicle membranes. An enriched synaptic vesicle fraction (LP2) was incubated with GTP $\gamma$ S or GDP (500  $\mu$ M) for 15 min at 37°C. His-GDI (5  $\mu$ M) or PBS (control) was added and the samples were incubated for an additional 45 min at 37°C. The membranes were then separated from the soluble fraction by centrifugation and analyzed by immunoblotting. While Rab3a was efficiently depleted from synaptic vesicles, Rab26 persisted on membranes. IB, immunoblotting. **(B)** Rab26 oligomerizes in a GDP-dependent manner. HEK293 cells transiently co-expressing EGFP-Rab26 variants (WT, QL, TN or NI) with FLAG-Rab26WT were lysed in detergent containing buffer followed by immunoprecipitation of EGFP-Rabs. Co-precipitation of FLAG-Rab26WT was observed with EGFP-Rab26 WT and even more efficiently with the GDP-preferring variant Rab26TN whereas co-precipitation with the nucleotide-empty variant (Rab26NI) was reduced and binding to the GTP-preferring variant (Rab26QL) was abolished. IP, immunoprecipitation. DOI: 10.7554/eLife.05597.005

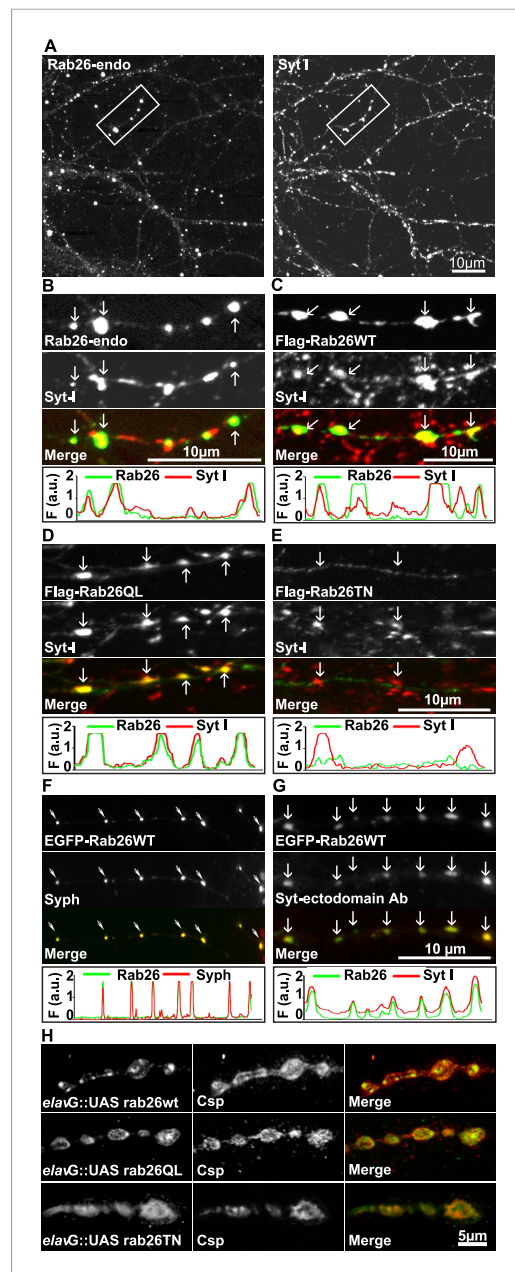


**Figure 3.** Endogenous and expressed GTP-Rab26 variants localize to a subset of synaptic vesicles in cultured hippocampal neurons. In (A–G), representative line scans of the two channels are shown below each set. In the y-axis, F (a.u.) indicates fluorescence intensity (arbitrary units). (A and B) Localization of endogenous Rab26 (detected with the newly generated monoclonal anti Rab26 antibody) and synaptotagmin 1 (Syt-I) in neurites of dissociated hippocampal neurons (DIV 15) reveals that Rab26 colocalizes with a subset of Syt-I positive puncta (B, arrows). (C–E) Expression of FLAG-tagged Rab26 variants in neurites (DIV 9 cultures 48hr after transfection). Both FLAG-Rab26WT (C) and QL (D) co-localize with a subset of synaptotagmin positive puncta (Syt-I), whereas FLAG-Rab26TN (E) exhibited

*Figure 3. continued on next page*

*Figure 3. Continued*

a more diffuse distribution. **(F)** Overexpression of EGFP-Rab26WT exhibits a distribution comparable to endogenous and FLAG-tagged Rab26 in neuritis where it colocalizes with synaptophysin (Syph). **(G)** Rab26-positive clusters contain actively recycling vesicles. Hippocampal cultures were incubated overnight with a labeled antibody directed against a luminal epitope of synaptotagmin (Syt1 clone 604.2 conjugated to Oyster-550), resulting in uptake during endocytosis. EGFP-Rab26WT is present in recycled synaptic vesicles as evident from the co-localization with synaptotagmin 1 positive puncta. **(H)** Localization of YFP-tagged Rab26 variants at the *Drosophila* neuromuscular junction (third instar larvae). The Rab26 variants (Rab26wt, GTP-preferring Rab26Q250L, and GDP-preferring Rab26T204N), were expressed using *elav-Gal4*. Neuromuscular junctions of third instar larvae expressing these Rab26 variants were stained with anti-GFP (green) and for endogenous cysteine string protein as vesicle marker (anti-Csp, red).

DOI: [10.7554/eLife.05597.006](https://doi.org/10.7554/eLife.05597.006)

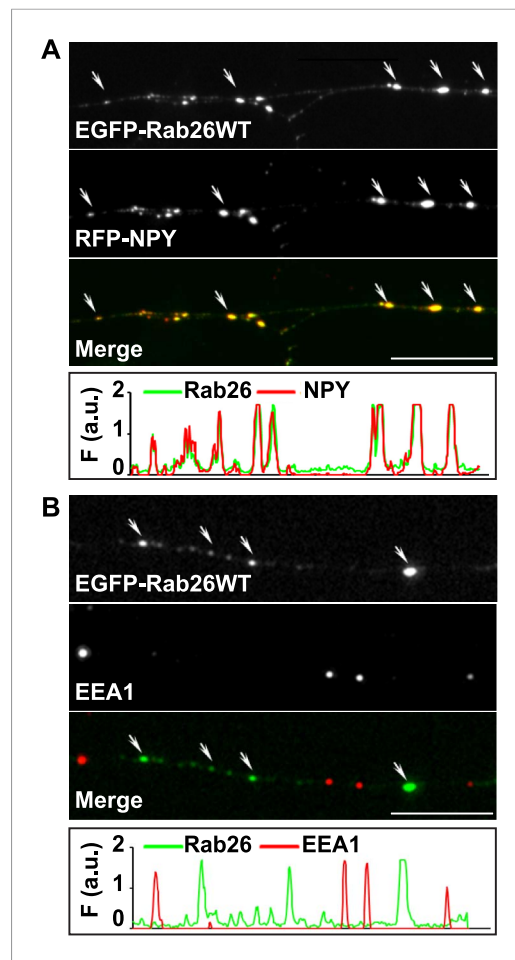


**Figure 3—figure supplement 1.** EGFP-Rab26WT colocalizes with the secretory neuropeptide Y (NPY) but not with EEA1 in neurites. **(A)** Hippocampal neurons (DIV 10) co-expressing EGFP-Rab26WT and RFP-NPY showed colocalisation of both proteins in neurites as indicated by the arrows. **(B)** No overlap was observed with the early endosomal marker EEA1 (arrows). Line scans beneath each figure shows extent of colocalization. Scale bars, 10  $\mu$ m.

DOI: [10.7554/eLife.05597.007](https://doi.org/10.7554/eLife.05597.007)

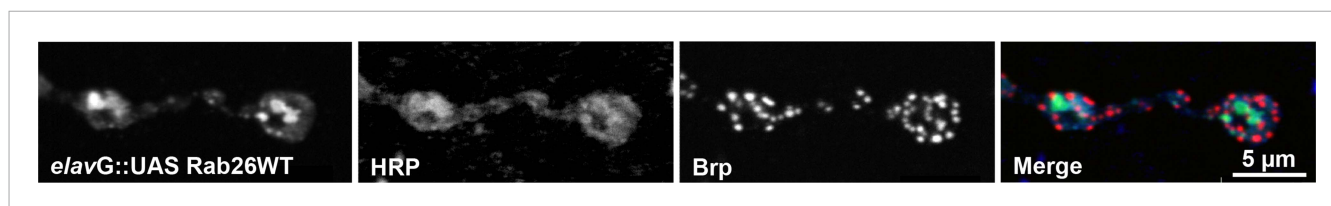


**Figure 3—figure supplement 2.** Rab26 does not colocalize with the presynaptic scaffold protein Brp in *Drosophila* neuromuscular junctions. YFP-tagged Rab26WT localizes to the presynaptic compartment of neuromuscular junctions (NMJs) in *Drosophila melanogaster* and forms huge structures that overlapped with the presynaptic membrane marker HRP, but not with the active zone marker Bruchpilot (Brp). The YFP tagged wild type Rab26 was expressed using the elav-Gal4 promoter. NMJs of larvae expressing YFP-Rab26WT were stained with anti-GFP (green), anti-HRP (blue) and anti-Brp (red). DOI: 10.7554/eLife.05597.008

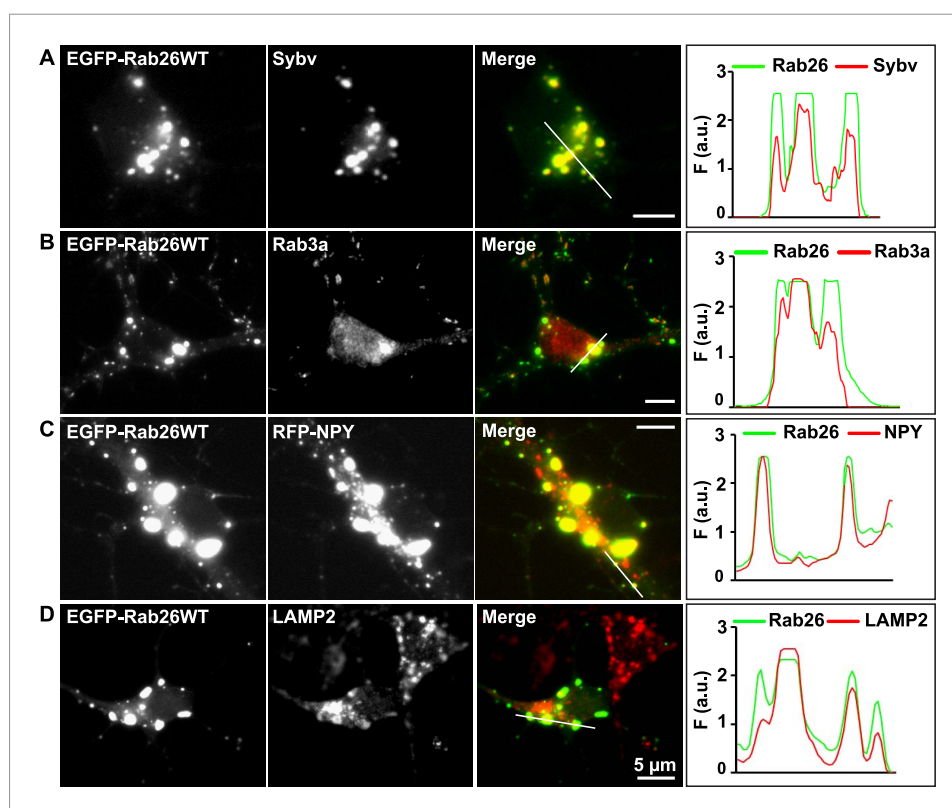


**Figure 4.** Expression of EGFP-Rab26 in cultured hippocampal neurons induces formation of large GFP-positive clusters in the neuronal cell bodies. (A–C): GFP-positive clusters colocalize with markers for synaptic and large dense core vesicles. (A and B) EGFP-Rab26 clusters contain synaptobrevin (Sybv) and Rab3a. (C) Co-expression of EGFP-Rab26WT with RFP-NPY results in almost complete overlap of both proteins in these clusters (C). (D) Partial overlap is also observable with the lysosomal membrane protein LAMP2. DIV 10, scale bar, 5  $\mu$ m. Line scans of select vesicle clusters (denoted by solid white lines in merged panel) signify the relative correlation between the individual fluorescent channels. F (a.u.) indicates fluorescence intensity (arbitrary units). DOI: 10.7554/eLife.05597.009



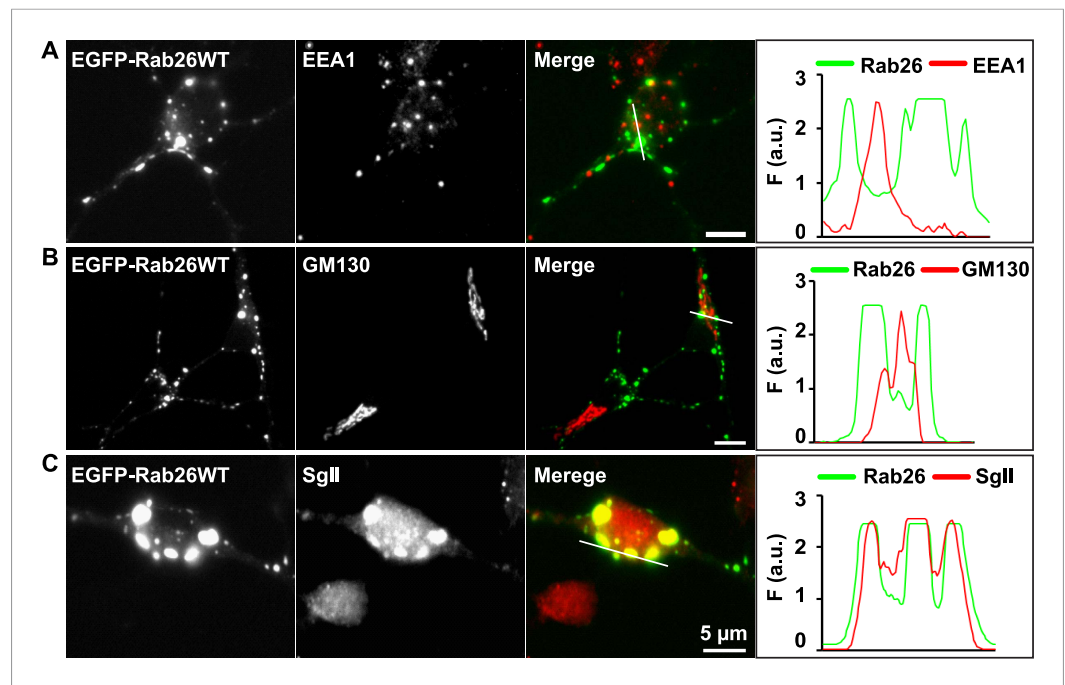


**Figure 4—figure supplement 1.** EGFP-Rab26WT colocalizes with the secretory protein secretogranin II but not with EEA1 and GM130 in neuronal somata. Hippocampal neurons (DIV 10) co-expressing EGFP-Rab26WT show no overlap between Rab26 and early endosomes (EEA-1) (A) or Golgi (GM130) (B) whose endogenous staining patterns are not affected by overexpression of EGFP-Rab26WT. In contrast, massive clustering of Secretogranin, SgII, a marker for large dense core vesicles (C) is observed, with the clusters perfectly colocalizing with EGFP-Rab26WT. Line scans adjacent of each figure shows the extent of colocalization.

DOI: [10.7554/eLife.05597.010](https://doi.org/10.7554/eLife.05597.010)

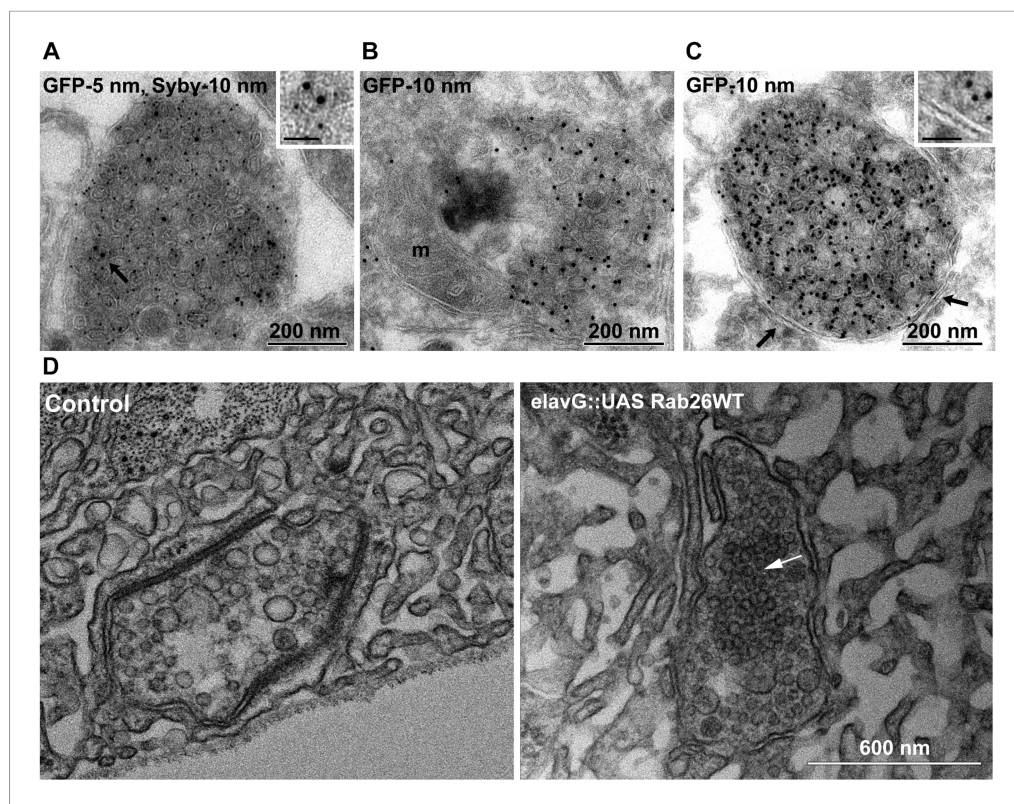


**Figure 5.** Ultrastructure of EGFP-Rab26 induced vesicle clusters in cultured hippocampal neurons and in neuromuscular junctions of *Drosophila* third instar larvae. (A–C) Ultrathin cryosections obtained from hippocampal neurons expressing EGFP-Rab26WT were immunogold labeled for EGFP and synaptobrevin (Sybv, monoclonal antibody 69.1 specific for synaptobrevin 2) and analyzed by electron microscopy. In the soma of hippocampal neurons organelles surrounded by one or two (C, inset, arrow) membranes were densely packed with small vesicles and very occasionally other organelles (e.g., mitochondria, m). Immunogold labeling for both EGFP and synaptobrevin was concentrated both on vesicles present inside and the surrounding membrane. Scale bar in insert, 50 nm. (D) Ultrathin sections of neuromuscular junctions obtained from *Drosophila* third instar larvae. Control animals show scattered vesicles of a somewhat heterogeneous size, typical for this developmental stage (Rasse *et al.*, 2005). Synapses of a strain expressing YFP-Rab26WT using the elavG::UAS system (elavG::UAS Rab26WT) display frequent clusters of densely packed vesicles (arrow) that are separated from the surrounding vesicles but lack a surrounding membrane.

DOI: [10.7554/eLife.05597.011](https://doi.org/10.7554/eLife.05597.011)

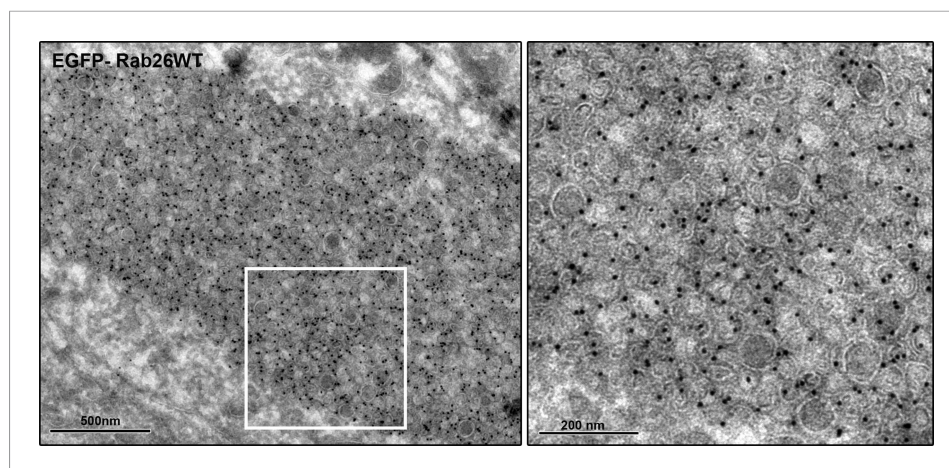


**Figure 5—figure supplement 1.** EGFP-Rab26 induces massive vesicle clustering in neuronal cell bodies. Ultrathin cryosections obtained from hippocampal neurons expressing EGFP-Rab26WT were immunogold labeled for EGFP and analyzed by electron microscopy. Transient expression of EGFP-Rab26WT results in the clustering of enormous numbers of vesicles positive for EGFP-Rab26.

DOI: [10.7554/eLife.05597.012](https://doi.org/10.7554/eLife.05597.012)



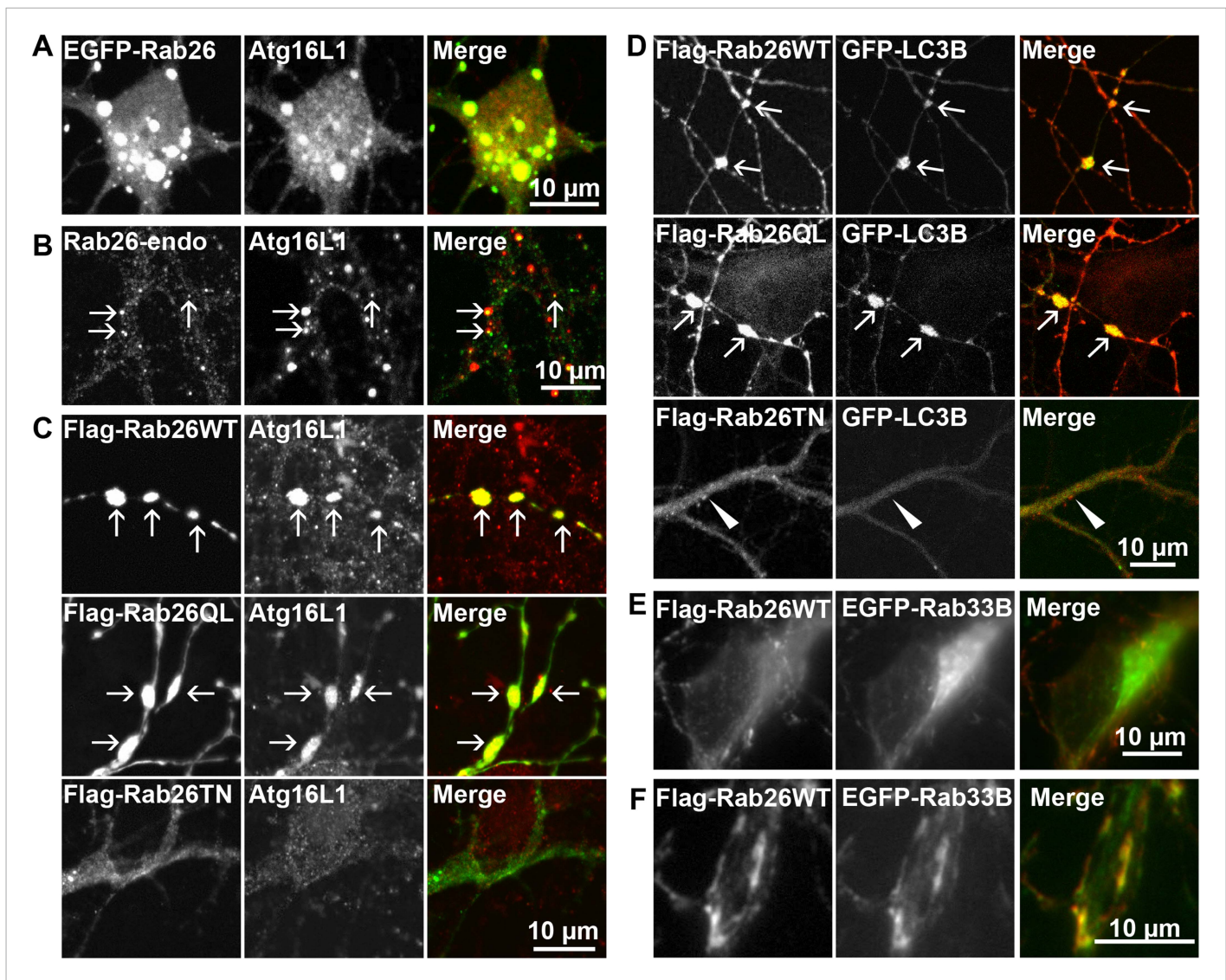


**Figure 6.** Clusters containing GTP-Rab26 colocalize with autophagosome-specific proteins both in cell bodies and dendrites of cultured hippocampal neurons. Arrows indicate co-localization. **(A)** Somatic clusters induced by expression of EGFP-Rab26WT co-localize with endogenous Atg16L1. **(B and C)** In neurites, Atg16L1 co-localizes with clusters of endogenous Rab26 (non-transfected, DIV 15, panel **B**) and with clusters containing FLAG-tagged Rab26WT and Rab26QL, but not with Rab26TN (transfected, DIV 9, panel **C**). **(D)** Similar colocalization patterns were obtained from neurites expressing FLAG-Rab26 variants and autophagosomes labeled by GFP-LC3B. Note that occasional puncta were observed for the GDP-preferring variant Rab26TN that, however, showed no overlap with LC3B (arrowhead). DIV 9. **(E and F)** Co-expression of FLAG-Rab26WT and EGFP-Rab33WT in hippocampal neurons. In the soma **(E)**, EGFP-Rab33 is primarily restricted to a perinuclear structure reminiscent of the Golgi apparatus whereas an almost perfect overlap was observed between the Rab33 and Rab26 in peripheral puncta lining neurites **(F)**. DIV 8.

DOI: [10.7554/eLife.05597.013](https://doi.org/10.7554/eLife.05597.013)

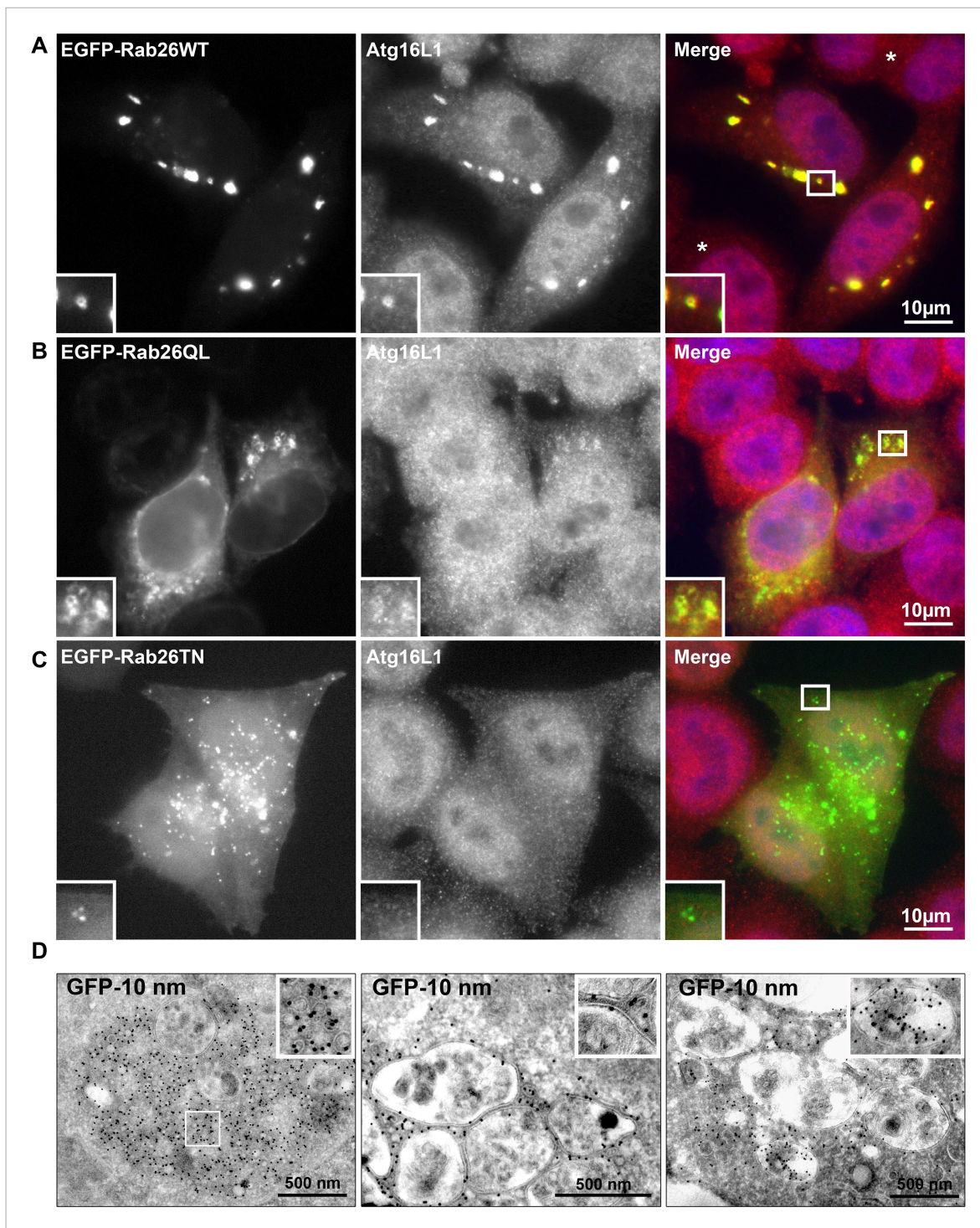


**Figure 6—figure supplement 1.** Rab26 overexpression causes vesicle clusters in HeLa. Endogenous ATG16L1 is recruited to vesicle clusters induced by transient overexpression of EGFP-tagged Rab26WT (A) or Rab26QL (B) in HeLa cells. Although GFP-Rab26TN forms small clusters in these cells, endogenous Atg16L1 is not recruited to these structures (C). (D) Immunogold electron microscopy analysis revealed that HeLa cells transfected with EGFP-Rab26WT exhibited formation of huge clusters of small vesicle (left panel, inset) that are sometimes surrounded by external membranes (right panel, inset) and large vacuole autolysosome-like compartments whose membrane were labeled with EGFP-Rab26WT (center and right panel). Rab26 was visualized by anti-GFP antibody coupled with 10 nm gold particles.

DOI: [10.7554/eLife.05597.014](https://doi.org/10.7554/eLife.05597.014)



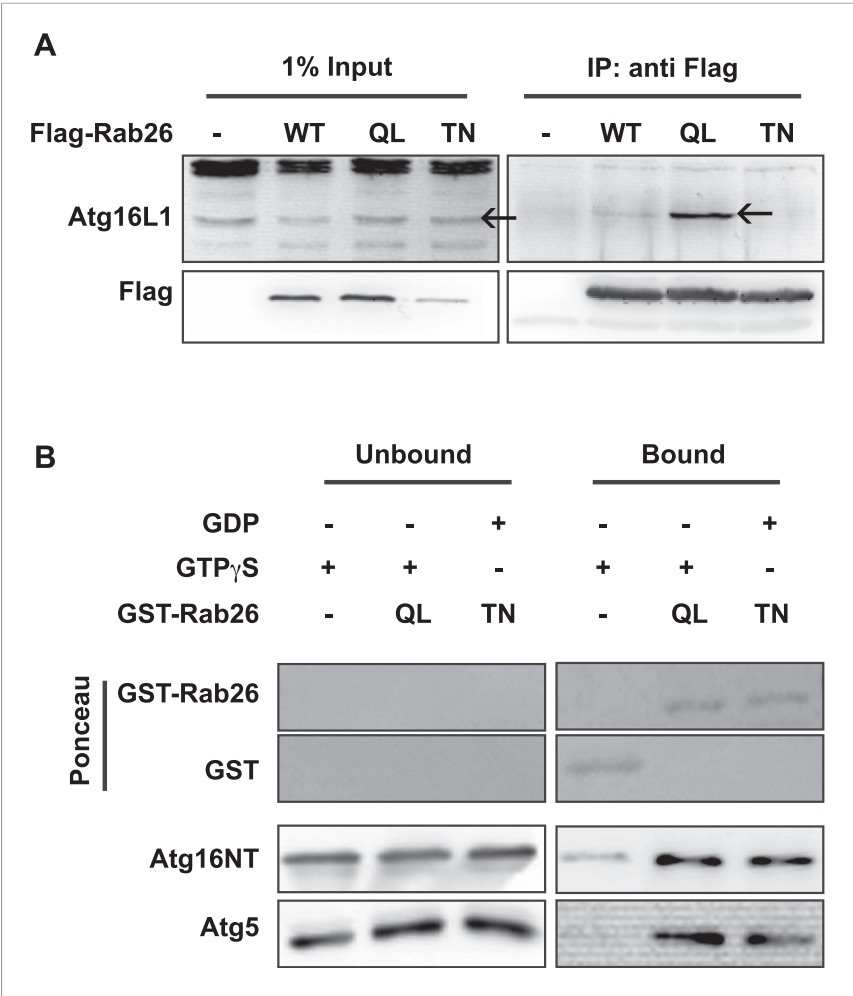


**Figure 7.** Atg16 is an effector of GTP-Rab26. **(A)** Co-Immunoprecipitation of FLAG-tagged Rab26 variants expressed in HeLa cells with endogenous Atg16L1 protein. Immunoprecipitation was carried out following lysis in detergent-containing buffer and clearance by centrifugation to remove cell debris. Note that only the GTP-preferring QL variant of Rab26 showed significant binding to Atg16L1 (arrow). **(B)** GST pulldown of purified recombinantly expressed GST-Rab26 variants with a pre-formed complex of His-tagged versions of Atg5 and the N-terminal domain of Atg16L1 (Atg16NT). Note that Atg16NT selectively interacted with the GTP-preferring QL-variant of Rab26. Furthermore, binding of Atg16NT to Rab26 resulted in the displacement of Atg5 from the preformed complex.  
DOI: [10.7554/eLife.05597.015](https://doi.org/10.7554/eLife.05597.015)

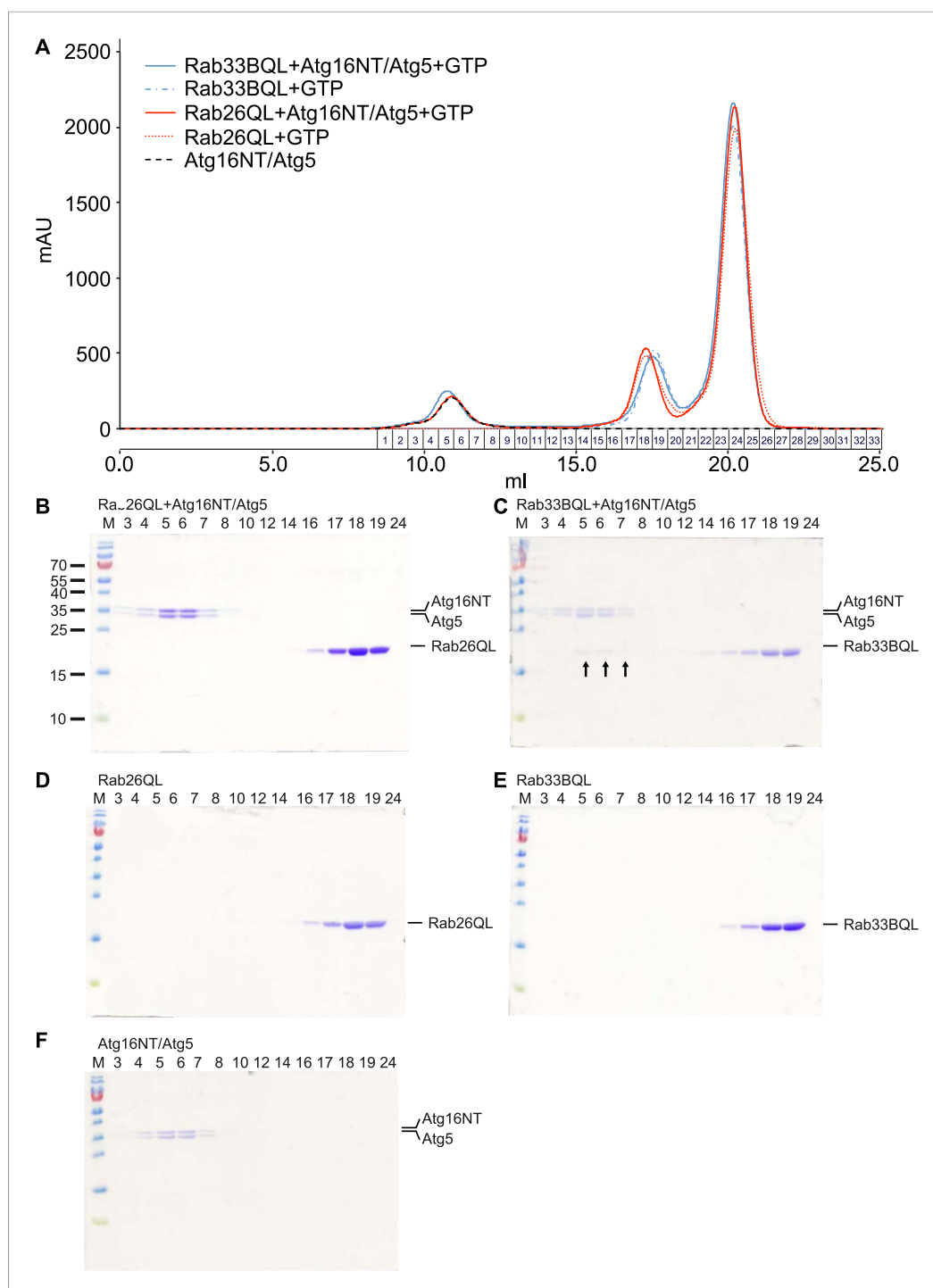


**Figure 7—figure supplement 1.** Analyses of Rab26 and ATG16L1 interaction by analytical gel filtration. To analyze complexes formed between Atg16L1 and Rab26 or Rab33, samples containing either Rab protein were pre-incubated with Atg16NT/Atg5 and loaded on a Superdex 200 10/30 GL column. As controls, Rab26, Rab33, or Atg16NT/Atg5 alone were separately loaded and analyzed. Eluted fractions were collected, analyzed by SDS-PAGE and protein bands visualized using Coomassie staining. **(A)** The elution profiles for various samples analyzed. **(B–F)** Representative fractions were separated on SDS PAGE gels and stained with Coomassie to visualize the protein bands. **(B)** Co-migration of Rab26QL with Atg16NT/Atg5 was not detected when pre-incubated samples of these proteins were tested. **(C)** Complexes of Rab33QL with Atg16NT/Atg5 can be observed to co-migrated (fractions 5–7, arrows). **(D–F)** Control runs were performed using only Rab26QL, Rab33QL or Atg16NT/Atg5.  
DOI: [10.7554/eLife.05597.016](https://doi.org/10.7554/eLife.05597.016)